

## Core-loss analysis of an (Fe, Co, Ni)-based nanocrystalline soft magnetic alloy

M. A. Willard<sup>a)</sup>

*U.S. Naval Research Laboratory, Code 6324, Washington DC 20375*

T. Francavilla

*GeoCenters Inc., Arlington, Virginia 22201*

V. G. Harris

*Electrical and Computer Engineering Department, Northeastern University, Boston, Massachusetts 02115*

(Presented on 8 November 2004; published online 10 May 2005)

Nanocrystalline soft magnetic materials possess higher magnetization and operation temperatures than amorphous alloys with similar compositions. For these reasons, they are good candidate materials for power electronics applications. As an indication of their performance, core losses have been measured for a nanocrystalline alloy with the composition  $\text{Fe}_{64.08}\text{Co}_{10.68}\text{Ni}_{10.68}\text{Zr}_{8.49}\text{B}_{4.86}\text{Cu}_{1.2}$  synthesized by a melt-spinning process with subsequent isothermal anneal at 550 °C for 1 h. The experiments were conducted on toroidal samples using a Walker ac permeameter over a frequency range of 100 Hz–500 kHz, at induction amplitudes of 100 and 1100 mT, at room temperature. A measured toroidal sample possessed a saturation magnetization of 1.529 T and core loss of 17.5 W/kg at a frequency of 10 kHz and magnetic flux density of 100 mT. The Steinmetz analysis of the static hysteresis losses yielded a power-law coefficient of 1.475. A statistical model for excess eddy current losses showed good agreement with experimental results. Excess eddy current losses were found to be the dominant factor in losses above 10 kHz for these alloys. © 2005 American Institute of Physics. [DOI: 10.1063/1.1847333]

Magnetic material core losses are a direct consequence of joule heating from electric currents induced in the material by the changing magnetization. By breaking down the total core loss into components based on the nature of the loss mechanism, we can better understand and reduce the overall losses. The most widely used method for partitioning has been to separate the losses into three portions: the static hysteretic loss, the classical eddy current loss, and the excess eddy current loss (sometimes referred to as anomalous or dynamic losses). The static hysteretic loss is determined by quasistatic hysteresis loop measurement and has origins in the localized Barkhausen jumps of domain walls. The classical eddy current loss is calculated from the fundamental equations of electromagnetics, assuming constant permeability and sinusoidal applied field. Finally, the excess eddy current loss has contributions from magnetic domain-wall dynamics with scales on the order of microstructural features.

In this paper, the separation of losses technique will be applied to a nanocrystalline soft magnetic material with the composition  $\text{Fe}_{64.08}\text{Co}_{10.68}\text{Ni}_{10.68}\text{Zr}_{8.49}\text{B}_{4.86}\text{Cu}_{1.2}$  in order to provide insight into the dominant loss characteristics in different frequency ranges. This alloy composition was expected to provide both low losses and high magnetization based on the characteristics of alloys with similar Fe, Co, and Ni compositions. As shown in this work, the excess eddy current loss dominates at frequencies above 10 kHz, where the potential application as a power electronics inductor component is most important.

An arc melter was used to form an ingot from elemental metals with purity exceeding 99.97%. The compositionally homogeneous ingot was then used to make ribbon samples by a single-wheel melt-spinning technique. An alloy with the composition  $\text{Fe}_{64.08}\text{Co}_{10.68}\text{Ni}_{10.68}\text{Zr}_{8.49}\text{B}_{4.86}\text{Cu}_{1.2}$  was produced using a wheel with a 50 m/s surface velocity and 0.76-mm crucible orifice. The resulting ribbons had an average thickness of 28  $\mu\text{m}$ , width of 2.1 mm, and up to a few meters in length.

The ribbon was wound onto a 14-mm-o.d. quartz tube and isothermally annealed in an argon atmosphere above the primary crystallization temperature to devitrify the samples. The toroid-shaped samples were then encased in epoxy and wrapped with primary and secondary windings for alternating current loss measurement. The toroid was annealed at 550 °C for 1 h in a furnace under a 100 cc/min flowing argon. The density of the material, as determined by gas pycnometry, was 7801 kg/m<sup>3</sup>. Other physical parameters are described in related works.<sup>1,2</sup>

Static hysteresis loops were measured using an ADE model 4HF vibrating-sample magnetometer. Short pieces of ribbon, 5–8 mm long, were measured at room temperature with maximum magnetic field values of 1.5, 3, 9, 12, 30, 50, and 1000 mT. The samples were oriented with the long axis in the direction of the applied magnetic field.

A Walker AHM-401 automatic hysteresisgraph was used to measure the core losses of the samples between 0.1 and 500 kHz. A sinusoidal wave form was used during the experiments at maximum flux density values of 100, 300, 500, 700, 900, and 1100 mT. Not all the data in these frequency

<sup>a)</sup>Electronic mail: willard@anvil.nrl.navy.mil

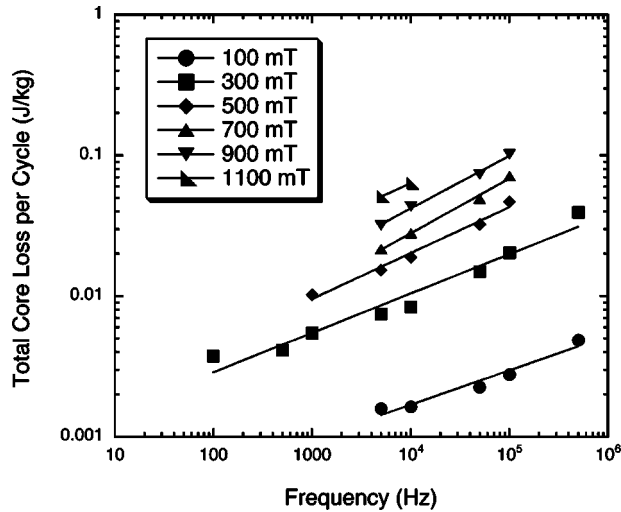


FIG. 1. Total core loss per cycle as a function of switching frequency for a  $\text{Fe}_{64.08}\text{Co}_{10.68}\text{Ni}_{10.68}\text{Zr}_{8.49}\text{B}_{4.86}\text{Cu}_{1.2}$  nanocrystalline alloy at various constant maximum flux densities.

and flux density ranges were of sufficient quality for analysis due to the wide range of reactance seen by the sample.

Figure 1 shows the measured total loss per cycle for a series of maximum applied flux densities. The total core losses measured for this alloy are comparable to those of a commercial amorphous alloy with the composition  $\text{Fe}_{78}\text{Si}_9\text{B}_{13}$  optimized for low losses.<sup>3</sup> The following analysis by separation of losses should provide insight into the important factors for reduction of losses in this nanocrystalline alloy.

As shown in Fig. 2, the static hysteresis loss per cycle  $P_h$  as a function of the maximum magnetic-flux density ( $B_{\text{max}}$ ) has a power-law relationship with the form

$$P_h = P_0 B_{\text{max}}^n, \quad (1)$$

where  $P_0$  is a fitting parameter for the hysteretic losses in J/kg. This relationship, found by Charles Steinmetz, typically

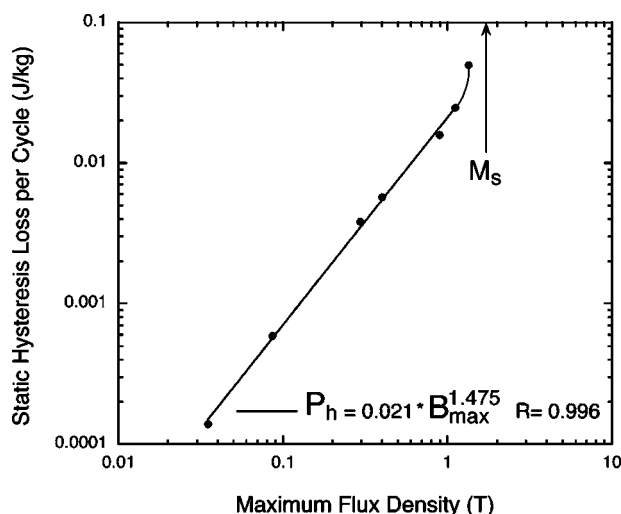


FIG. 2. Static hysteresis loss per cycle as a function of maximum flux density measured by vibrating sample magnetometry. The fit to the curve follows a Steinmetz power law with  $P_0=0.021$  and  $n=1.475$ . The saturation magnetization was previously published in Ref. 2.

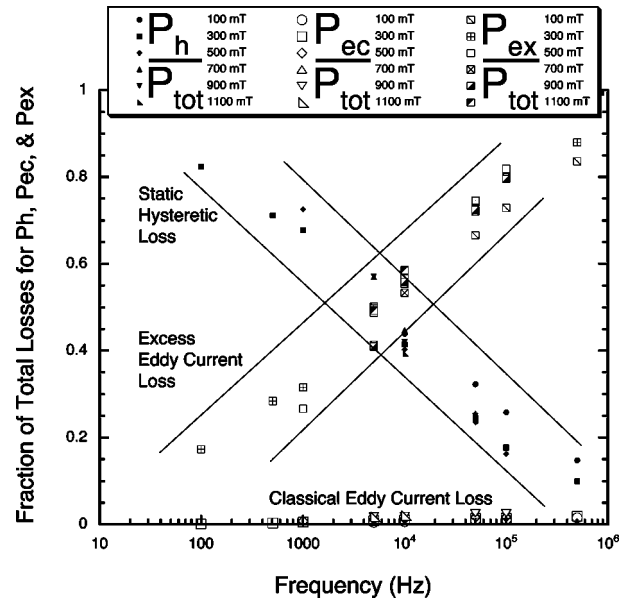


FIG. 3. Fraction of the total losses represented by static hysteresis, classical eddy currents, and excess eddy currents as a function of frequency. The hysteretic losses are dominant at low frequencies, while the excess eddy current losses dominate at high frequencies.

exhibits an exponent ( $n$ ) between 1.5 and 1.6 for maximum flux densities exceeding about 50 mT.<sup>4</sup> Near saturation, deviations from this power law are observed, as indicated in Fig. 1 by the upward rise in hysteresis loss at the maximum flux densities above 1 T.

The dynamic losses, found at higher frequencies, are isolated from the static hysteretic losses by subtraction based on the Steinmetz analysis. The classical eddy current losses are computed in loss per cycle for the case when the thickness of the laminate is much greater than the skin depth.<sup>5</sup> Under constant permeability and sinusoidal applied field conditions, the classical eddy current loss equation has the form

$$\frac{P_{\text{ec}}}{f} \cong \frac{\pi^{3/2} t B_{\text{max}}^2 \sqrt{f}}{2\sqrt{\mu\rho_e}}, \quad (2)$$

where  $t$  is the ribbon thickness,  $\mu$  is the permeability of the specimen,  $\rho_e$  is the resistivity ( $45 \mu\Omega \text{ cm}$ ), and  $f$  is the switching field frequency.

The analysis of the losses was carried out by separation of the total core loss into static hysteretic, classical eddy current, and excess eddy current components. A Steinmetz analysis was performed on the core losses of the hysteresis loops measured by vibrating-sample magnetometry. The Steinmetz analysis of this alloy provided the parameters  $P_0=0.021$  J/kg and  $n=1.475$ . These values are similar to 4% Si-steel samples across the measured range of maximum flux density.<sup>4</sup>

The eddy current component of the losses was then isolated from the static part by subtraction. Using Eq. (2), the classical eddy current loss was calculated. Finally, the excess eddy current loss was isolated by subtraction of the classical eddy current loss from the total eddy current loss

The fractions of the total loss corresponding to hysteretic, classical, and excess eddy current losses are presented as a function of the switching field in Fig. 3. As one might

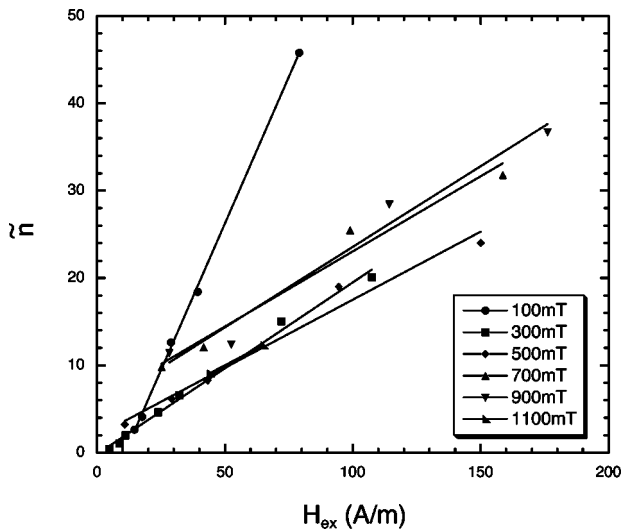


FIG. 4. Number of active switching regions as a function of the excess field, as determined by a statistical model for excess eddy current loss. The slope is related to microstructural features of the sample and is equal to  $1/V_0$ .

expect, the hysteretic loss dominates at low frequency. The classical eddy current losses never make up a large part of the total loss due to the skin effects at high frequencies. Excess eddy current losses make up the majority of the loss above 10 kHz. This is similar to amorphous alloys, however it is quite different than electrical steels.<sup>6,7</sup>

A statistical loss theory has been applied to the excess eddy current loss as a tool to understand these losses that dominate at high frequencies. As developed by Bertotti *et al.*, this theory considers the magnetization switching of a lamination with cross section  $S$  and number of randomly arranged active flux switching regions  $\tilde{n}$ .<sup>8,9</sup> The increase to the width of the dynamic hysteresis loop produced by domain-wall effects is embodied in the excess field  $H_{ex}$ . This quantity is determined experimentally by the relation

$$H_{ex} = \frac{P_{ex}}{4B_{max}f}, \quad (3)$$

where  $P_{ex}$  is the excess eddy current loss found by the separation of losses described above. The excess field is related to  $\tilde{n}$  by considering a case where all of the switching occurs at a single  $180^\circ$  domain wall following the form:

$$H_{ex} = \frac{H^{(w)}}{\tilde{n}} = \frac{4G^{(w)}SB_{max}f}{\rho_e\tilde{n}}, \quad (4)$$

where  $H^{(w)}$  is the switching field for the single planar domain wall and  $G^{(w)}=0.1356$  is a geometric factor describing the same.

Considering this analysis,  $\tilde{n}$  has been calculated by the ratio of  $H^{(w)}$  to  $H_{ex}$  as illustrated in Fig. 4. For each maximum applied flux density, the data are found to be nearly linear in  $H_{ex}$  and with the slope nearly independent of  $B_{max}$  above 100 mT. This is a similar result to previous studies on

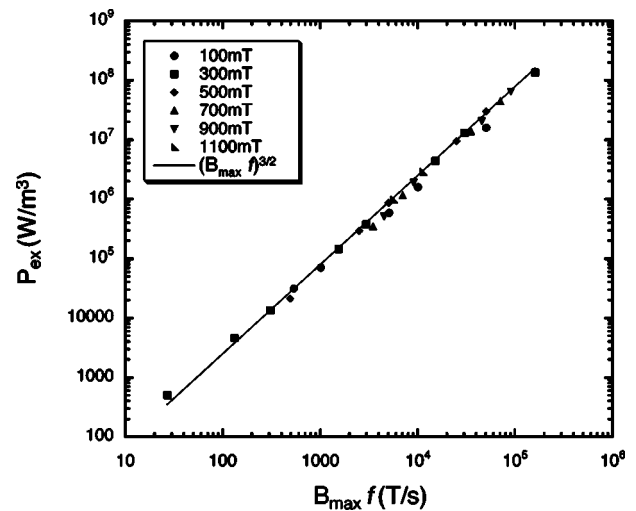


FIG. 5. The excess eddy current loss as a function of the product of maximum induction and switching frequency. The fit line represents a power law of  $3/2$  with a proportionality factor equal to  $8\sqrt{G^{(w)}SV_0/\rho_e}$ .

other soft magnetic materials,<sup>7</sup> where  $\tilde{n}=n_0+(1/V_0)H_{ex}$ , and  $V_0$  is a hypothetical magnetic field controlled by the microstructure of the material. The data for  $B_{max}$  at 100 mT have a much steeper slope indicating that there are more active regions for switching in the hysteresis loop. This may account for the significantly smaller total losses as seen in Fig. 1.

When the excess eddy current loss is plotted as a function of the product of the maximum flux density and switching frequency, as shown in Fig. 5, the resulting power law is very close to  $3/2$  (solid line). Using Eqs. (3) and (4) in conjunction with the  $V_0$  relationship described above (neglecting the contribution of  $n_0$  as small), the proportionality factor for the power law can be calculated. The proportionality factor is determined to be  $8\sqrt{G^{(w)}SV_0/\rho_e}$ , which yields values between 2.45 and 2.76 for the values of  $V_0$  shown in Fig. 4. The excellent fit to the data in Fig. 5 was found for a proportionality factor of  $5/2$ .

Two of the authors (M.A.W. and T.F.) gratefully acknowledge the support of the Office of Naval Research. The authors would also like to thank Dr. Jeff Long for assistance with gas pycnometry measurements.

<sup>1</sup>M. A. Willard, J. H. Claassen, R. M. Stroud, and V. G. Harris, J. Appl. Phys. **91**, 8420 (2002).

<sup>2</sup>M. A. Willard, J. C. Claassen, R. M. Stroud, T. L. Francavilla, and V. G. Harris, IEEE Trans. Magn. **38**, 3045 (2002).

<sup>3</sup>K. Suzuki, A. Makino, A. Inoue, and T. Masumoto, J. Appl. Phys. **70**, 6232 (1991).

<sup>4</sup>R. M. Bozorth, *Ferromagnetism* (IEEE, New York, 1978), pp. 509–510.

<sup>5</sup>G. Bertotti, *Hysteresis in Magnetism* (Academic, New York, 1998) pp. 391–430.

<sup>6</sup>C. D. Graham Jr., J. Appl. Phys. **53**, 8276 (1982).

<sup>7</sup>K. J. Overshott, IEEE Trans. Magn. **MAG-17**, 2698 (1981).

<sup>8</sup>G. Bertotti, F. Fiorillo, and G. P. Soardo, IEEE Trans. Magn. **MAG-23**, 3520 (1987).

<sup>9</sup>G. Bertotti, IEEE Trans. Magn. **24**, 621 (1988).